Advances in Bioresearch
Adv. Biores., Vol 15 (5) September 2024: 126-136
©2024 Society of Education, India
Print ISSN 0976-4585; Online ISSN 2277-1573
Journal's URL:http://www.soeagra.com/abr.html
CODEN: ABRDC3
DOI: 10.15515/abr.0976-4585.15.5.126136

Advances in Bioresearch

ORIGINAL ARTICLE

Study of Intermolecular Interaction between 6-Gingerol and Egg white Proteins: Improved Solubility and Stability, Combined Anti-inflammatory Effect by Molecular Docking studies

Anuradha D Otari[1]*, Rupali A. Patil[2], Chandrashekhar D. Upasani[1]
[1]SNJB's Shriman Sureshdada Jain College of Pharmacy, Chandwad, Nashik-423101, M.S. India
[2]MGV's Pharmacy College, Panchavati, Nashik-422003, M.S., India
*Corresponding Author: anugavade2008@gmail.com

ABSTRACT
This work examines the molecular interactions between 6-gingerol, a bioactive component of ginger, and egg white proteins with special emphasis on improving 6-gingerol solubility and stability. Also, the study focuses on combined anti-inflammatory potentialities of 6-gingerol with lysozyme and the outcomes from TLR4 and TNF-α pathways interactions. An attempt was made to further understand the molecular interactions of 6-gingerol with the major egg white proteins such as ovalbumin and lysozyme via molecular docking experiment. The effect of these proteins on 6-gingerol solubility and the effect on its stability were determined by mimicking the interaction with these proteins. The feasibility of a synergistic anti-inflammatory activity of 6-gingerol with lysozyme was also analysed using the molecular docking study with TLR4 and TNF-α profiles. Computer aided molecular docking analysis showed considerable interactions between 6-gingerol and egg white proteins especially ovalbumin which improves the aqueous solubility and stability of 6-gingerol. In addition, molecular docking analysis revealed that there is the enhancement of the anti-inflammatory activity when 6-gingerol is combined with lysozyme in the TLR4 and TNF-α pathways. The present study emphasizes the fact that egg white proteins particularly ovalbumin can optimally improve the solubility and stability of 6-gingerol. Furthermore, it has been found that the possibility of enhancement of anti-inflammatory properties of 6-gingerol and lysozyme in a synergistic manner through TLR4 and TNF-α pathway. These results may have potential developments to enhance the effectiveness of the therapeutic action of 6-gingerol in states of inflammation using protein-protein interactions.
KEY WORDS: Molecular docking, 6-Gingerol, Solubility, Stability, Synergism, Anti-inflammatory activity.

Received 04.06.2024 Revised 21.07.2024 Accepted 21.09.2024

How to cite this article:
Anuradha D O, Rupali A. P, Chandrashekhar D. U. Study of Intermolecular Interaction between 6-Gingerol and Egg white Proteins: Improved Solubility and Stability, Combined Anti-inflammatory Effect by Molecular Docking studies. Adv. Biores. Vol 15 [5] September 2024. 126-136

INTRODUCTION

The studies of the cross section of natural structures and biomolecules give much information concerning matters of remedy and function. Of such compounds gingerol, a member of the ginger (*Zingiber officinale*) family of bioactive components, has drawn interest due to its pharmacological properties, which include anti-inflammatory, antioxidant, and anticancer activities [1]. Studying how gingerol binds to proteins will help to define the given compound's action mechanisms and create new opportunities for its usage in medicine and diet [2]. Egg white proteins such as ovalbumin, ovotransferrin, Lysozyme and ovomucoid are very well known for their functional and biological characteristics. These proteins are involved in different essential physiological functions and hence find use in food industry and pharmaceuticals [3]. Depending on the type of the small molecules, they can have a strong impact on functional properties and stability of the bioactives, for example gingerol present in ginger.

Molecular docking is a versatile computational approach that helps to anticipate the molecular interaction between two binding partners, including drug and target biomolecule, at the molecular level [4]. Significance of docking study is tremendous to understand various aspects related with drug as: 1)

Molecular docking is useful in helping explain the mode of interaction between different molecules, or between a given molecule and one target molecule. Thus, through the mimicry of such interactions, it is possible to study the patterns of synergistic effects. 2) In docking studies, the researchers are in a position to find out which of the molecules complements the other in producing Synergy effects. Through the analysis of the binding affinities and the interactions profile, it is possible to determine if two compounds may act synergistically or antagonistically to another or if two groups of compounds have an additive effect. When learning about synergism which is the state whereby the outcome of a reaction due to an interaction of two or more compounds is more than the independent totals of the compounds, molecular docking is quite useful. When evaluating the interaction index—this is the effect which occurs when the impact of two or more compounds is greater than the cumulative impact of the lesser effects. 3) The knowledge of the phenomenon helps to set more efficient treatment plans for optimizing Drug Design. With docking, it is possible to develop drugs which when administered in combination point to different pathways or receptors, thus increasing the efficacy of the treatment. 4) Molecular docking is able to significantly decrease the number of experimental combinations that must be prepared on the level of the compound synthesis since it offers the first approximation of the synergistic effects. This can be less time-consuming and cost effective, tapering the pointless experiments on far away contenders. 5) Since docking studies deliver data on atomic level, the comparison of synergistic interactions might provide information on better efficacy or decreased toxicity. Findings from this study may be beneficial for analysis of multiple interactions in systems biology and pharmacology. 6) Molecular docking extends the efficiency and efficacy of prediction and optimization of solubility precisely owing to the understanding of the molecular interactions. It aids in the choice of effective and selective solubilizers, proper formulation in the delivery of drugs and that of the properties of the drugs to enhance solubility thus leading to the development of efficient and effective drugs [5]. In this case, through docking of gingerol with egg white proteins, we have got information relative to the binding affinities and interaction sites as well as the potential change in protein conformation. This study also assists in the elucidation of the biological actions of 6-gingerol at the molecular level as well as improving functional foods and potential therapeutic agents. In the present investigation we make use of molecular docking to understand the binding profile of 6-gingerol with major egg white proteins. The goal for this study is to define the binding modes in order to understand if it could have functional consequences on the structure and function of the interactors. Possible implications of the results of this study may strengthen the current knowledge of 6-gingerol impact on the protein activity and contribute to the discovery of novel beneficial uses in wellness and feeding.

MATERIALS AND METHODS

Target Protein Retrieval and Preparation

Ovalbumin's (PDB ID 1OVA) X-ray crystallographic structures were obtained from the RCSB Protein Data Bank [6] and validated using a number of factors, including resolution, mutation, co-crystal ligand, wwPDB Validation, and Ramachandran plot according to the information below**.**

Table 1: Comparison between standard values and retrieved protein for validation of protein Selected for docking study

Parameters	Details	Standards
Protein Id	1VOA	-
Method of experiment	X-RAY Diffraction	X-RAY Diffraction
Mutation	No	No
Resolution	1.95 Å	Near about 3.00 Å
wwPDB Validation	Better	Better
Co-Crystal Ligand	Absent	-
Ramchandran Plot (by PROCHECK server) Residues in favoured + Allowed regions	90.1 %	>88 %

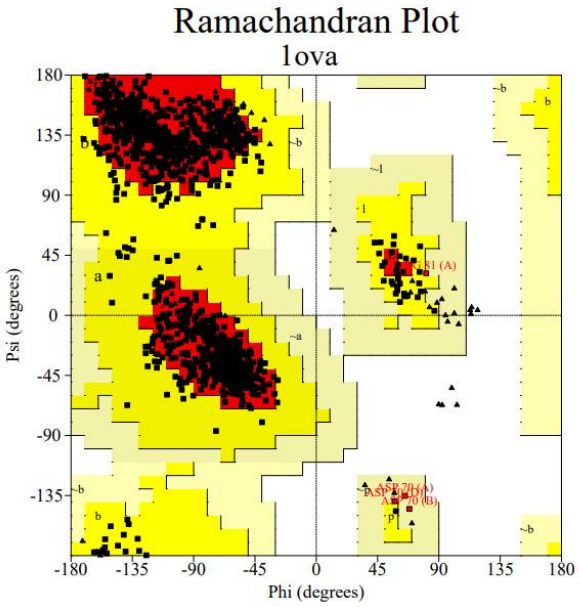

Figure 1. Ramachandran Plot 1OVA obtained from PROCHECK server

CHIMERA v1.16 was utilized for the structural optimization and minimization of proteins. It included force fields for standard (AMBER ff14SB) and nonstandard (AM1-BCC) residues [7]. As a result, all nonstandard residues, such as water molecules and cocrystal ligands, as well as superfluous chains, were eliminated from the proteins. Based on a comprehensive review of existing literature, our research focused on investigating key targets associated with **Anti-inflammatory**, including TNF-α, Toll-like receptor (TLR4-human), Tetragonal Hen egg white lysozyme [8]. To do this we utilized the National Center for Biotechnology Information (NCBI) service to fetch the fasta sequences for the Homo sapiens taxon in question [9]. Third, the identified proteins were searched through the Protein Data Bank (PDB) for the presence of similar biological sequences with the aid of Basic Local Alignment Search Tool (BLAST) [10]. A rigorous selection of the top 5 to 10 sequences was made using criteria including E-value, % identity, and query coverage. Next, we obtained the three-dimensional X-ray crystallographic structures of TNF-α, Toll-like receptor (TLR4-human), and Tetragonal Hen egg white lysozyme from the PDB database using their respective accession numbers [11]. The existence of co-crystal ligands, resolution, mutation analysis, wwPDB validation, and evaluation of the Ramachandran plot were among the criteria used to validate these structures [12]. Here are the specifics.

Table 2: Comparison between standard values and retrieved protein for validation of protein Selected for docking study

Parameters	**Protein details**			**Standards**
Targets	**TNF-α**	**TLR-4**	**Hen egg white lysozyme**	-
Protein id	2AZ5	3FXI	2YVB	-
Method of experiment	X-ray diffraction	X-ray diffraction	X-ray diffraction	X-ray diffraction
Mutation	No	No	No	No
Resolution	2.10 Å	3.10 Å	1.62 Å	Near about 2.00 a^0
Wwpdb validation	Better	Better	Better	Better
Co-crystal ligand	307	--	--	-
Ramchandran plot **(**by procheck server) Residues in favoured + allowed regions	90.2%	100%	100%	>80 %

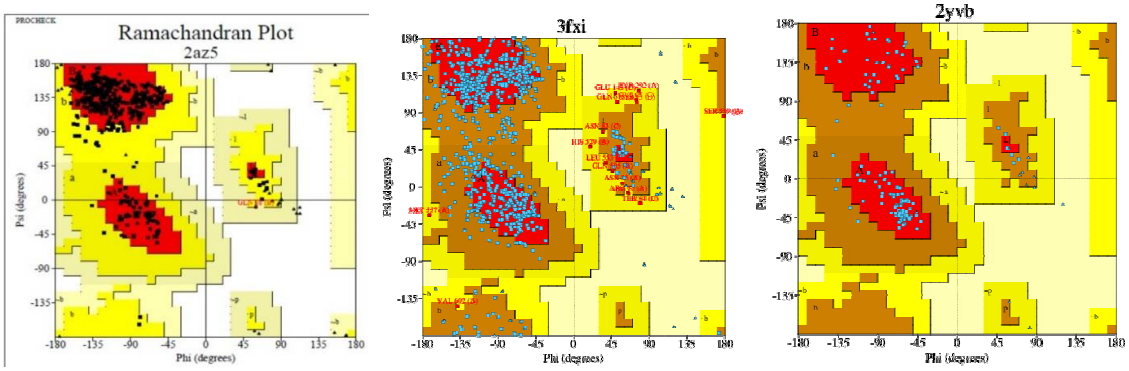

Figure 2. Ramachandran Plot 2AZ5, 3FXI & 2YVB obtained from PROCHECK server

Before conducting docking studies, it is crucial to optimize and minimize the molecules, whether they are macromolecules or macromolecules [13]. To ensure the accuracy of our research, we first verified the residues within the binding pockets of the proteins from the PDBsum server. PDBsum is a visual library of 3D Protein Data Bank structures that provide details on how typical inhibitors and proteins interact [14]. To prepare the proteins for docking studies, we addressed missing residues and generated side chains using CHIMERA v1.16. Subsequently, optimization and minimization procedures were applied [15]. One thousand steepest descent steps with a steepest descent size of 0.1 Å were used in the optimization procedure. These steps were followed by one hundred conjugate gradient steps with a 0.1 Å size [16]. Furthermore, we made sure that all hydrogen atoms including the slower ones were supplied and that histidine's protonation states were established [17]. By utilizing the AMBER ff14SB force field, charges were added. Using Biovia Discovery Studio Visualizer V21.1.0.20298, any nonstandard residues, such as water molecules and extraneous chains, were eliminated from the proteins after optimization and reduction [18].

Grid Generation

AutoDockTools 1.5.6 [19], Chimera 1.11 [20], and Maestro Version 12.7.161 were employed for grid Generation and validation Grid Parameters were obtained using orientation of co-crystal ligand or CASTp server if protein in Apo state.

Table 3: The active sites amino acids

Protein ID	The active sites amino acids
1OVA	HIS44, HIS45, ALA46, ASN47, GLU48, ASN49, ILE50, ASP151, GLN152, ARG154, GLU155, LEU156, ASN158, SER159, GLU162, SER163, ASN166, GLY167, ILE168, ILE169, ARG170, ASN171, VAL172, GLN174, PRO175, VAL189, PHE190, LYS191, LYS199, ASP200, GLU201, THR203, GLN204, ALA205, MET206, PRO207, ARG209, VAL210, THR211, GLU212, GLN213, GLU214, SER215, LYS216, PRO217, VAL218, GLN219, PRO255, GLU256, VAL257, SER258, GLY259, LEU260, GLU261, GLU264, ARG290, MET291, LYS292, MET293, GLU294, GLU295, LYS296, TYR297, ALA335, HIS337, GLU339, ILE340, ASN341, GLU342, ALA343, HIS368, PRO369, ARG387, VAL389, SER390, PRO391, GLU40, LEU41, LYS42, ALA150, LEU173, SER176, SER177, VAL178, ALA197, PHE198, ASN298, SER301, VAL302, GLN331, ALA332, VAL333, GLY344, VAL347, GLY24, SER25, ILE26, GLY27, ALA28, MET31, SER59, MET63, LEU84, PRO85, GLY86, PHE87, GLY87, ILE87, GLN87, CYS87, THR88, SER89, VAL90, ASN91, SER94, SER95, ARG97, ASP98, ILE99, LEU100, ASN101, GLN102, ILE103, THR104, LYS105, PRO106, ASN107, ASP108, VAL109, TYR110, SER111, PHE112, SER113, LEU114, ALA115, SER116, GLN132, LYS135, GLU136, LEU137, TYR138, ARG139, GLY140, GLY141, TRP160, GLN164, LEU193, GLU195, LYS196, LEU226, PHE227, ARG228, GLU241, PRO243, PHE244, SER245, GLY246, THR247, SER249, LEU251, PHE269, LEU272, THR273, THR276, SER277, SER278, ASN279, MET281, GLU281, ARG345, GLU346, CYS373, LYS375, HIS376, ILE377, ALA378, THR379, ASN380, VAL382, ALA60, SER87, ALA87, ARG117, TYR119, GLU122, PRO128, LEU131, LEU142, GLU143, PRO144, ILE145, ASN146, ALA149, ALA153

PROTEIN ID	*THE ACTIVE SITES AMINO ACIDS*
1OVA	*HIS44, HIS45, ALA46, ASN47, GLU48, ASN49, ILE50, ASP151, GLN152, ARG154, GLU155, LEU156, ASN158, SER159, GLU162, SER163, ASN166, GLY167, ILE168, ILE169, ARG170, ASN171, VAL172, GLN174, PRO175, VAL189, PHE190, LYS191, LYS199, ASP200, GLU201, THR203, GLN204, ALA205, MET206, PRO207, ARG209, VAL210, THR211, GLU212, GLN213, GLU214, SER215, LYS216, PRO217, VAL218, GLN219, PRO255, GLU256, VAL257, SER258, GLY259, LEU260, GLU261, GLU264, ARG290, MET291, LYS292, MET293, GLU294, GLU295, LYS296, TYR297, ALA335, HIS337, GLU339, ILE340, ASN341, GLU342, ALA343, HIS368, PRO369, ARG387, VAL389, SER390, PRO391, GLU40, LEU41, LYS42, ALA150, LEU173, SER176, SER177, VAL178, ALA197, PHE198, ASN298, SER301, VAL302, GLN331, ALA332, VAL333, GLY344, VAL347, GLY24, SER25, ILE26, GLY27, ALA28, MET31, SER59, MET63, LEU84, PRO85, GLY86, PHE87, GLY87, ILE87, GLN87, CYS87, THR88, SER89, VAL90, ASN91, SER94, SER95, ARG97, ASP98, ILE99, LEU100, ASN101, GLN102, ILE103, THR104, LYS105, PRO106, ASN107, ASP108, VAL109, TYR110, SER111, PHE112, SER113, LEU114, ALA115, SER116, GLN132, LYS135, GLU136, LEU137, TYR138, ARG139, GLY140, GLY141, TRP160, GLN164, LEU193, GLU195, LYS196, LEU226, PHE227, ARG228, GLU241, PRO243, PHE244, SER245, GLY246, THR247, SER249, LEU251, PHE269, LEU272, THR273, THR276, SER277, SER278, ASN279, MET281, GLU281, ARG345, GLU346, CYS373, LYS375, HIS376, ILE377, ALA378, THR379, ASN380, VAL382, ALA60, SER87, ALA87, ARG117, TYR119, GLU122, PRO128, LEU131, LEU142, GLU143, PRO144, ILE145, ASN146, ALA149, ALA153*

Table 4: Active Sites Amino Acids

Protein	Active Sites Amino Acids
2AZ5	LEU57A, TYR59A, SER60A, TYR119A, LEU120A, GLY121A, GLY122A, TYR151A, LEU57B, TYR59B, SER60B, TYR119B, LEU120B, GLY121B, TYR151B, LEU55D

The box was designed to be as small as possible to maintain conformity to the expected docking of ligands and the structure and properties of the active site of the protein. To identify receptor grids, three programs were used: AutoDockTools, Chimera, and Maestro. The size of the grid for the proteins that have co-crystal ligands was defined by the measurement of the ligand and for the proteins that do not possess co-crystal ligands, the equivalent volume was extracted from the CASTp server. SPPIDER and META-PPISP servers [21]. The information about amino acids found in the grid pocket is as follows.

Table 5. Grid parameter Ovalbumin

Sr.no	Protein Id	Centre Coordinates			Size Coordinates		
		x	y	z	X	y	z
1	**1OVA**	1.773	49..846	39.916	35	35	35

Table 6. Grid Parameter

PDB ID	Centre co-ordinates			Size co-ordinates		
	X	**Y**	**Z**	**X**	**Y**	**Z**
2AZ5	-19.41	-74.65	33.85	25	25	25

The size of the enclosing box was kept small in order to maintain conformity to the size and shape of the ligands that were expected to dock and the structure and nature of the protein active site.

Ligands Preparation

Ligands were taken out of ChemSpider and imported into MarvinSketch underwent 2D and 3D cleaning. Cleaned Structures then subjected to MMFF94 force field for minimization [23], and the conformer with the lowest energy was chosen for further study in MOL2 format. The targeted molecule was then conducted in MarvinSketch v21. 13 washed in 2D and 3D, optimized with MMFF94 force field and the conformation with lowest energy was chosen. This gave the 3D mol2 file format which was then saved.

Molecular Docking Of Target Protein with Ligands

After getting the desired ligands and proteins, an internal script developmed with auto dock tools version 1. 5. 6 for ligands and ADF were suit for proteins was applied to change all the structures from pdb to pdbqt [19]. This script retained all of the receptors as rigid objects while all the bonds in the ligands were free to rotate or move. We used the AutoDock Vina 1. 2. 3 for docking research in our molecular docking simulations, separating grid points by 0. 375 ˚A. The computer could search for other places where ligands and receptors might bind because the grid box was placed at the target's active site. Other configurations were therefore regarded as the standard. The values of XYZ coordinates in the Table No. 3 was following with other parameters like CPU 23, exhaustiveness 32 number of modes 9 and energy range three. For the redocking the subjects used the similar scenarios as the ones used in the earlier dockings.

Ligand and Protein acquisition

Initially, the 3D structures of the ligand and protein were obtained through internet search and were converted through an internal bash shell script developed by the writers using AutoDock tools 1. 5. 7 for ligands and ADFRsuit for proteins from which pdbqt format is generated [23]. Rigid receptor was assumed here but this script allowed all rotatable bonds of the ligands to rotate. As afforded by the grid step size of 0. 375 A and Auto Dock vina 1. 2. 5, we proceeded to explore the chances of docking with our preferred ligands. This was made possible since the grid box was focused on the target active spot as indicated above, and the software could look for other potential regions, where ligand and receptors may interact [24]. That is why other setups were considered normal. They are fixed as the following specifics from the Table No. 3: Grid Box Dimensions: X = 50m; Y = 100m; Z = 200m; X:Y:Z coordinates – 100;200;5 respectively. The modes were nine and energy levels were divided into three groups, other settings CPU was 23 and for energy 32 [25]. The configurations used for the previously completed dockings were used for redocking.

Protein-protein docking

The utilization of molecular docking allows involving two biomolecules together in which they form a complex structure, the conformation of which corresponds to the molecular biology and, in the ideal, the conformation of the original complex. 2YVB is docked with ClusPro where 3FXI was considered as receptor and 2YVB is the ligand [26]. To ensure that protein-protein interaction is constrained to the interacting site, docking servers predict interface residues.

Visualization

The graphical output for the protein-ligand docking results for Gingerol bound to the 2AZ5 structure was then viewed in likely mode using the Biovia Discovery Studio visualizer; this led to creation of images of 2D and 3D images & and Maestro 13.1 while results from ClusPro were subjected to PDBsum for protein-protein interaction. The Biovia Discovery Studio visualizer was used to create a complex out of the results of the Autodock Vina processing. Maestro 12. 3 was applied to make 2D & 3D images for complexes [27](academic edition). Next, we obtained the three-dimensional X-ray crystallographic structures of TNF-α, Toll-like receptor (TLR4-human), and Tetragonal Hen egg white lysozyme. From the PDB database using their respective accession numbers [28]. The current framework used to validate these structures included the presence of co-crystal ligands, resolution, mutation analysis, wwPDB validation, and evaluation of the Ramachandran plot. Here are the specifics.

RESULTS AND DISCUSSION

Docking Score and intermolecular interactions of ligands with Protein VEGFR-2 (1OVA) PLIP. The provided table presents binding energy and cluster Score of intermolecular interactions of Gingirol with TNF-α (2AZ5) using the PLIP server and Hen egg white lysozyme (2YVB) with TLR-4 (3FXI) using the PDBsum server. These include hydrogen bonds, salt bridges and hydrophobic interactions; other information is the residue identification number and distance.

Table 7: Docking Score and intermolecular interactions of ligands with Protein VEGFR-2 (1OVA) PLIP.

Protein-Ligand Docking				
Name of compound	Binding Energy	Type of Interaction	Residue ID	Distance
1OVA_Gingerol	-5.107	Hydrophobic Interactions	LYS105C	3.88
			PRO106C	3.73
			PRO106C	3.88
			ARG139D	3.82
		Hydrogen Bonds	THR104D	2.48
			LEU114D	1.86
			LEU114D	2.62

Table 8: binding energy and cluster Score of intermolecular interactions of Gingirol with TNF-α (2AZ5) using PLIP server and Hen egg white lysozyme (2YVB) with TLR-4 (3FXI) using PDBsum server.

Protein-Ligand Docking					
Sr. No	Name of compound	Binding Energy	Type of Interaction	Residue ID	Distance
1	6-Gingerol	-5.587	Hydrophobic Interactions	LEU57A	3.59
				TYR59A	3.46
				TYR59A	3.82
				TYR59B	3.78
				TYR59B	3.62
				TYR119A	3.82
				TYR151A	3.94
			Hydrogen Bonds	GLY121A	2.62
Protein-Protein Docking					
2	Hen egg white lysozyme	-960.5	H-Bonds	AGLU31-BARG128, AASP60-BARG14, AGLU336-BARG73, AARG355-BSER72, AARG382-BASP101, ATYR403-BTRP62, AASP405-BTRP62, AGLN430-BARG112, AASP453-BARG112, ASER455-BARG112, AHIS456-BLYS116, AASP502-BARG112, AGLN505-BLYS116, AASN526-BASN113, AHIS529-BLYS116, AASP550-BARG114, AGLN578-BGLY117, AGLU603-BTRP123, AGLU605-BARG125,	
			Non-bonded Interactions	AGLU31-BARG128, AVAL32-BALA10, APRO34-BARG128, AGLN39-BARG14, AASP60-BARG14, AHIS334-BARG73, AGLU336-BARG73, AARG355-BGLY71, ATHR357-BARG73, ATHR359-BTRP62, APHE377-BGLY71, AASP379-BTRP62, ASER381-BTRP62, AARG382-BASP101, ATYR403-BARG61, AASP405-BTRP62, AHIS426-BASP48, AGLN430-BARG112, AILE450-BTHR47, AASP453-BARG112, ASER455-BARG112, AHIS456-BLYS116, AGLU474-BTHR47, AALA479-BARG112, APHE500-BVAL109, AASP502-BASN113, ASER504-BASN113, AGLN505-BARG112, AASN526-BASN113, ASER528-BASN113, AHIS529-BLYS116, AVAL548-BARG114,	

				AASP550-BARG114, ALEU553-BARG114, AGLN578-BGLY117, AGLU603-BTRP123, AGLU605-BARG125, AARG606-BALA122
			Salt-bridge	AGLU42-BARG128, AASP60-BLYS13, AASP84-BLYS13, AHIS179-BASP119, ALYS230-BASP119, AGLU266-BLYS33, AGLU336-BLYS116, AASP379-BARG112, AASP502-BARG73

Interface statistics

It may assist to utilize an interior script developed with AutoDock tools 1. 5, the structures were modified to pdbqt after the ligands and proteins were obtained. This makes six ligands and one ADFRsuit for each of the proteins. This script gave freedom to all the rotatable bonds of the ligands while the receptors were considered rigid. For the docking investigations in the present study, AutoDock Vina version 1 was employed apart with the grid points denoted as Grid_3, Grid_2, and Grid_1 respectively. Since in grid box the active site of the target was located at the center the computer could look for other place where the ligand and the receptor could join. In the other pictures, setups were included that were only considered typical. The same environment that was utilised for the dockings was also used for the redockings.

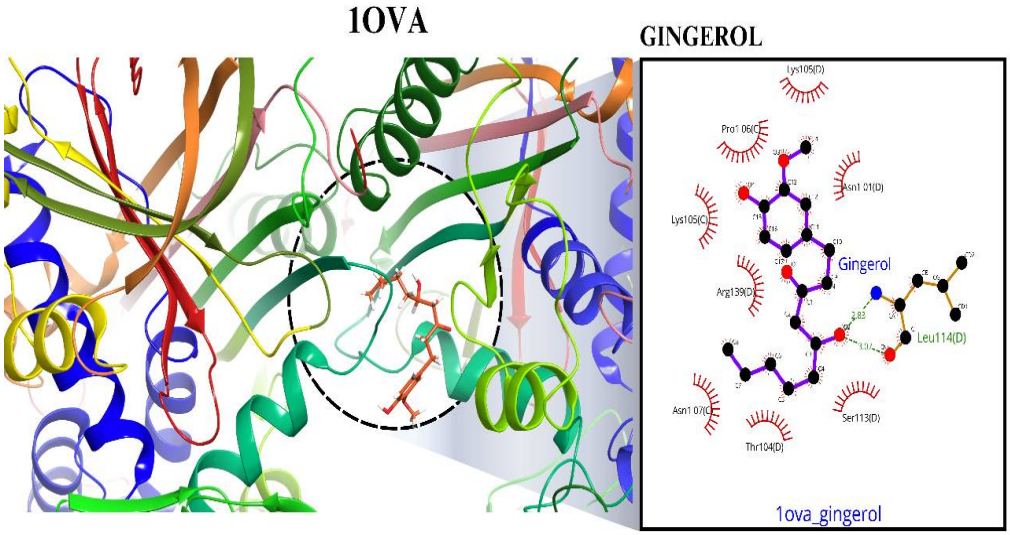

Figure 3. Molecular docking 2D and 3D images and ligplot of the Gingirol with Ovalbumin using LigPlot v1.4.5 and Maestro V12.8.

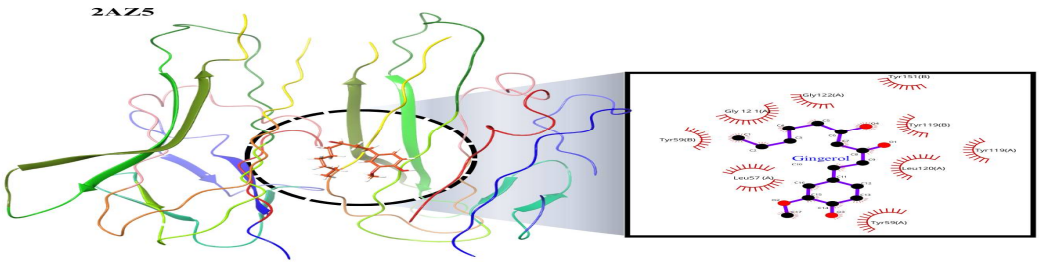

Figure 4. Molecular docking 2D and 3D images and ligplot of the Gingirol with TNF-α (2AZ5) using LigPlot v1.4.5 and Maestro V12.8.

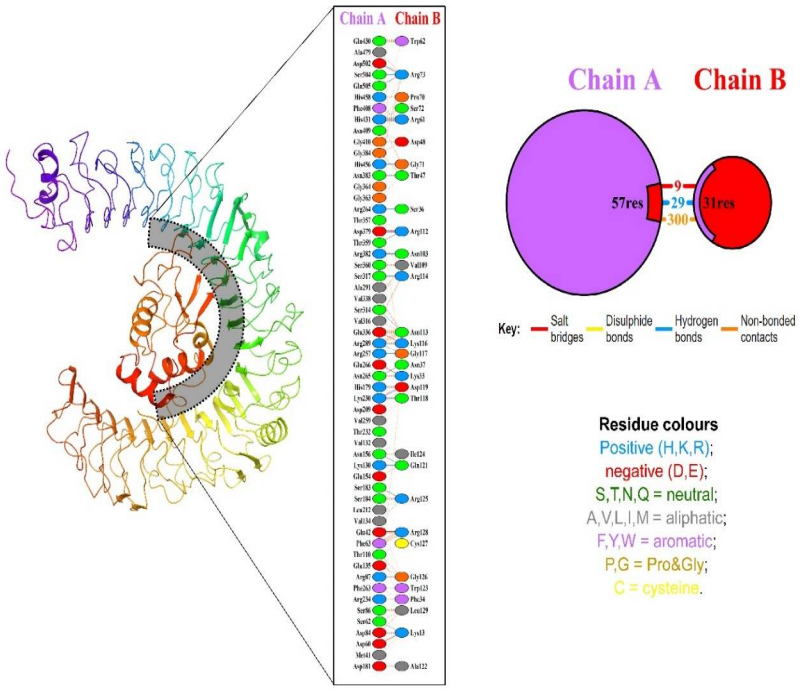

Figure 5: Molecular docking 2D and 3D images of Hen egg white lysozyme (2YVB) with TLR-4 (3FXI).

Table 9: interface statistics of Hen egg white lysozyme (2YVB) with TLR-4 (3FXI)

Chain	No. of interface residues	Interface area (Å²)	No. of salt bridges	No. of disulphide bonds	No. of hydrogen bonds	No. of non-bonded contacts
A	57	1673	9	---	29	300
B	31	1997				

CONCLUSION

The negative binding enegry, presence of both hydrophobic interactions, and a hydrogen bond suggest a robust and specific binding of 6 Gingerol to ovalbumin suggest enhanced solubility and stability of gingerol with ovalbumin. The negative binding energy, presence of both hydrophobic interactions, and a hydrogen bond suggest a robust and specific binding of Gingerol to TNF-α (2AZ5) and Hen egg white lysozyme **(**2YVB) with TLR-4 **(**3FXI**).** The stability of the complexes depended on the residues participating in hydrophobic interactions such as salt bridges and hydrogen bonds. The docking score reinforces the notion of a strong binding affinity, indicating the potential effectiveness of both complexes. This study presents a novel insight into the synergistic anti-inflammatory potential of the combination therapy using 6-Gingirol and Hen egg white lysozyme. Through molecular docking studies, we have identified significant interactions between Gingerol and TNF-α, as indicated by a binding energy of -5.587, and between Hen egg white lysozyme and TLR-4, with a notable cluster score of -960.5. These findings suggest a robust binding affinity and potential inhibitory effects on key inflammatory pathways. TNF-α and TLR-4 are well-established mediators in the inflammatory cascade, playing pivotal roles in the activation and perpetuation of inflammatory responses. The interaction of 6-Gingirol with TNF-α and Hen egg white lysozyme with TLR-4 could imply a dual mechanism of action in mitigating inflammation. Gingirol's interaction with TNF-α suggests a direct modulation of this cytokine's activity, potentially reducing its pro-inflammatory signaling. Concurrently, the binding of Hen egg white lysozyme to TLR-4 could interrupt the initial steps of the inflammatory pathway, offering an upstream inhibitory effect. The combination therapy's strength lies in its ability to target different, yet complementary, aspects of the inflammatory response. This dual approach could potentially offer a more comprehensive anti-inflammatory effect compared to monotherapy. The synergistic effect observed in this study underscores the potential of this combination therapy in providing a more effective and perhaps a more controlled response in treating inflammatory conditions. Our study lays the groundwork for future clinical

investigations to validate these findings in vivo and explore the therapeutic potential of this combination in clinical settings. Further research is essential to understand the pharmacokinetics and pharmacodynamics of this combination, along with its safety profile in clinical scenarios. The 6-Gingirol and Hen egg white lysozyme combination emerges as a promising therapeutic strategy in the realm of anti-inflammatory treatments. This study enhances our understanding of the molecular interactions at play and sets the stage for future explorations into its clinical applicability and potential benefits in managing inflammatory disorders.

REFERENCES

1. Zhang, M., Zhao, R., Wang, D., Wang, L., Zhang, Q., Wei, S., & Wu, C. (2021). Ginger (Zingiber officinale Rosc.) and its bioactive components are potential resources for health beneficial agents. *Phytotherapy Research*, *35*(2):, 711-742.
2. Gokara, M., Yusuf Zamal, M., Lavudiya, V. S., & Subramanyam, R. (2024). Deciphering the binding mechanism of gingerol molecules with plasma proteins: implications for drug delivery and therapeutic potential. *Journal of Biomolecular Structure and Dynamics*, 1-18.
3. Li, Z., Huang, X., Tang, Q., Ma, M., Jin, Y., & Sheng, L. (2022). Functional properties and extraction techniques of chicken egg white proteins. *Foods*, *11*(16):, 24-34.
4. Pagadala, N. S., Syed, K., & Tuszynski, J. (2017). Software for molecular docking: a review. *Biophysical reviews*, *9*, 91-102.
5. Pinzi, L., & Rastelli, G. (2019). Molecular docking: shifting paradigms in drug discovery. *International journal of molecular sciences*, *20*(18):, 4331.
6. Berman, H. M., Westbrook, J., Feng, Z., Gilliland, G., Bhat, T. N., Weissig, H., & Bourne, P. E. (2000). The protein data bank. *Nucleic acids research*, *28*(1):, 235-242.
7. Pettersen, E. F., Goddard, T. D., Huang, C. C., Couch, G. S., Greenblatt, D. M., Meng, E. C., & Ferrin, T. E. (2004). UCSF Chimera—a visualization system for exploratory research and analysis. *Journal of computational chemistry*, *25*(13):, 1605-1612.
8. Drexler, S. K., Sacre, S. M., & Foxwell, B. M. (2006). Toll-like receptors: a new target in rheumatoid arthritis? *Expert review of clinical immunology*, *2*(4):, 585-599.
9. Coordinators, N. R. (2013). Database resources of the national center for biotechnology information. *Nucleic acids research*, *41*(Database issue), D8.
10. Donkor, E. S., Dayie, N. T., & Adiku, T. K. (2014). Bioinformatics with basic local alignment search tool (BLAST) and fast alignment (FASTA). *Journal of Bioinformatics and sequence analysis*, *6*(1):, 1-6.
11. Ramos, J., Laux, V., Haertlein, M., Forsyth, V. T., Mossou, E., Larsen, S., & Langkilde, A. E. (2021). The impact of folding modes and deuteration on the atomic resolution structure of hen egg-white lysozyme. *Acta Crystallographica Section D: Structural Biology*, *77*(12):, 1579-1590.
12. Burley, S. K., Berman, H. M., Duarte, J. M., Feng, Z., Flatt, J. W., Hudson, B. P., ... & Zardecki, C. (2022). Protein data bank: a comprehensive review of 3D structure holdings and worldwide utilization by researchers, educators, and students. *Biomolecules*, *12*(10):, 1425.
13. Abdelsattar, A. S., Dawoud, A., & Helal, M. A. (2021). Interaction of nanoparticles with biological macromolecules: A review of molecular docking studies. *Nanotoxicology*, *15*(1):, 66-95.
14. Adebiyi, M. O., & Obagbuwa, I. C. (2024). Homology Modeling and Binding Site Analysis of SARS-CoV-2 (COVID-19) Main Protease 3D Structure. In *Research Anthology on Bioinformatics, Genomics, and Computational Biology*, 933-947.
15. [15]. Pettersen E. F., Goddard T. D., Huang C. C., Couch G. S. , Greenblatt D.M., Meng E. C., (2004) UCSF Chimera--a visualization system for exploratory research and analysis. J. Comput Chem. 25(13):,1605-1612.
16. Kaappa, S., Del Río, E. G., & Jacobsen, K. W. (2021). Global optimization of atomic structures with gradient-enhanced Gaussian process regression. *Physical Review B*, *103*(17):, 174114.
17. Girame, H., Garcia-Borràs, M., & Feixas, F. (2022). Changes in protonation states of in-pathway residues can alter ligand binding pathways obtained from spontaneous binding molecular dynamics simulations. *Frontiers in Molecular Biosciences*, *9*, 933-947.
18. Mousavi, H., Zeynizadeh, B., & Rimaz, M. (2023). Green and efficient one-pot three-component synthesis of novel drug-like furo [2, 3-d] pyrimidines as potential active site inhibitors and putative allosteric hotspots modulators of both SARS-CoV-2 MPro and PLPro. *Bioorganic Chemistry*, *135*, 106390.
19. Eberhardt, J., Santos-Martins, D., Tillack, A. F., & Forli, S. (2021). AutoDock Vina 1.2. 0: New docking methods, expanded force field, and python bindings. *Journal of chemical information and modeling*, *61*(8):, 3891-3898.
20. https://www.chemspider.com/Chemical-Structure.4445106.html
21. Trott, O., & Olson, A. (2009). Software news and update AutoDock Vina: Improving the speed and accuracy of docking with a new scoring function. *Effic. Optim. Multithreading*, *31*, 455-461.
22. Salentin, S., Schreiber, S., Haupt, V. J., Adasme, M. F., & Schroeder, M. (2015). PLIP: fully automated protein–ligand interaction profiler. Nucleic acids research,43(W1):, 443-447.
23. Zuhri, U. M., Purwaningsih, E. H., Fadilah, F., & Yuliana, N. D. (2022). Network Pharmacology integrated molecular dynamics reveals the bioactive compounds and potential targets of *Tinospora crispa* Linn. as insulin sensitizer. *Plos one*, *17*(6):, e0251837.

24. Rosell, M., & Fernández-Recio, J. (2020). Docking-based identification of small- molecule binding sites at protein-protein interfaces. *Computational and structural biotechnology journal*, *18*, 3750-3761.
25. Naumann, T., & Matter, H. (2002). Structural classification of protein kinases using 3D molecular interaction field analysis of their ligand binding sites: target family landscapes. *Journal of medicinal chemistry*, *45*(12):, 2366-2378.
26. Alekseenko, A., Ignatov, M., Jones, G., Sabitova, M., & Kozakov, D. (2020). Protein–protein and protein–peptide docking with ClusPro server. *Protein Structure Prediction*, 157-174.
27. Yang, S., Kar, S., & Leszczynski, J. (2023). Tools and software for computer-aided drug design and discovery. In *Cheminformatics, QSAR and Machine Learning Applications For Novel Drug Development* (pp. 637-661). Academic Press.
28. Laskowski, R. A., Jabłońska, J., Pravda, L., Vařeková, R. S., & Thornton, J. M. (2018). PDBsum: Structural summaries of PDB entries. *Protein science*, *27*(1), 129-134.